INVESTIGATING THE VIABILITY OF A CARBON NANOTUBE SURFACE AS A GASTRIC CANCER SCREENING TOOL

by

BRI MCALLISTER

A THESIS

Presented to the Department of Biology
and the Robert D. Clark Honors College
in partial fulfillment of the requirements for the degree of
Bachelor of Science

June, 2020

An Abstract of the Thesis of

Bri McAllister for the degree of Bachelor of Arts
in the Department of Biology to be taken June, 2020

Title: Investigating the Viability of a Carbon Nanotube Surface as a Gastric Cancer Screening Tool

Approved: *Dr. Benjamín Alemán*
Primary Thesis Advisor

Gastric cancer is a type of cancer that affects the stomach, esophagus, and duodenum. According to the American Cancer society, there were an estimated 27,510 diagnosed cases in the US, 2019 (American Cancer Society, 2019). Although this value only represents about 1.8% of all cancer sites in 2019, there was a low 40.5% survival rate of those diagnosed. Its presence is often asymptomatic until reaching advanced stages of the disease. When symptoms of indigestion, nonspecific stomach pain, anorexia, weight loss or early satiety are expressed, it's easy to confuse the cause with other ailments. By the time they were officially diagnosed, around 50% of patients' cancer had progressed beyond the locoregional area. Of those who had the disease in the locoregional area, only 50% could have a curative removal of the diseased tissue3. Current diagnostic techniques for gastric cancer include endoscopy and a barium swallow study. Endoscopy is a highly invasive and costly procedure used to investigate suspicious gastric, esophageal and duodenal lesions. Any sample that appears suspicious is biopsied and examined, and often has a 70% sensitivity for diagnosing the existing cancer. If there are six additional biopsies from the margin and base of the initial sample, sensitivity jumps to 98% (Graham, DY, 1982). A barium swallow study is an

imaging technique using barium and x-rays to image the upper gastrointestinal tract. This image allows for potential identification of malignant ulcers and lesions in the esophagus, stomach, and duodenum. Any abnormal findings require a follow up endoscopic examination. In comparison to endoscopy, a barium study is significantly less invasive. However, this test tends to produce up to 50% false negatives in various cases (Dooley, CP, 1984). The aim of this study is to evaluate the effectiveness in gastric cancer cell capture rate in a single-walled carbon nanotube (CNT) forest substrate. To test the differences in gastric cancer capture rate, we patterned a silicon oxide substrate with a checkerboard carbon nanotube surface using photolithography and chemical vapor deposition. We seeded cell lines AGS (ATCC: CRL-1739) and KATO III (ATCC: HTB 103) onto this surface in decreasing densities and counted the overall capture rate on both silicon oxide and CNT squares. Our results indicated no significant difference in KATO III capture rate and significance in two densities of AGS. Overall, the results indicate that there may be preferential entrapment at a specific density range for fully adherent gastric cancer cells and that this experiment should be repeated to test if these results are replicable.

Acknowledgements

I would like to thank Professor Aleman, Professor Zemper, and Bree Mohr for helping me to investigate the properties of carbon nanotubes, gastric cancer, and to learn various lab techniques related to this thesis. I'm thankful for having the opportunity to explore my potential as a research scientist and to ask my own questions. I appreciate all of the guidance and encouragement I've been given in answering my research questions. I owe all of my growth to those who have mentored me and inspired me to pursue a career in science, and to those who showed it was within my capabilities to grow into a scientist. I'd like to thank my Thesis Committee assistant professor Benjamin Aleman, assistant professor Anne Zemper, and professor of practice Barbara Mossberg. The support I've received from Robert D. Clark Honors College has been incredible, and I'm glad to have been pushed outside of my comfort zone and guided to grow as an academic. I'd like to finish by thanking my family for providing emotional strength and assurances when I grew frustrated during the process of researching and writing for this thesis. I don't think I wouldn't have been able to finish this without those words of love.

Table of Contents

List of Figures

Introduction

A profile of gastric cancer

Gastric cancer is one of the more common cancer worldwide, with an estimated 1.0 million cases in 2018 (*Global Cancer* Observatory, 2018). Its incidence rate in the US has decreased over the last few decades to an estimated predication of 27,600 cases in 2020 (*American Cancer* Society, 2020). The average age of those diagnosed with cancer is 68, and 6 of 10 people diagnosed are 65+ (Tierney, Lawrence M. etal, 1999)). Men tend to be diagnosed with it twice as often as women are.

Gastric cancer affects the esophagus, stomach and the duodenum, with the stomach as the most commonly affected site in the GI tract (Papaxoinis, George, et. Al., 2006). The exact causes of gastric cancer are currently unknown, but there are a few risk factors associated with the disease. One of the stronger risk factors is the presence of *H pylori* bacteria. In an analysis of 12 case control studies, *H pylori* infection had been shown to be strongly associated with non-cardia gastric cancer, increasing the risk almost six-fold (*Gut,* 2001). Other risk factors include obesity, anemia, family history of gastric cancer, alcohol, smoking and red meat consumption (Zali, Hakimeh, et al., 2011). According to *Current: Medical Diagnosis and Treatment*, its morphology can be characterized in variety of types: ulcerating masses; polypoid or fungating intraluminal masses; linitis plastica; and superficial spread (Tierney, Lawrence M. et. Al.).

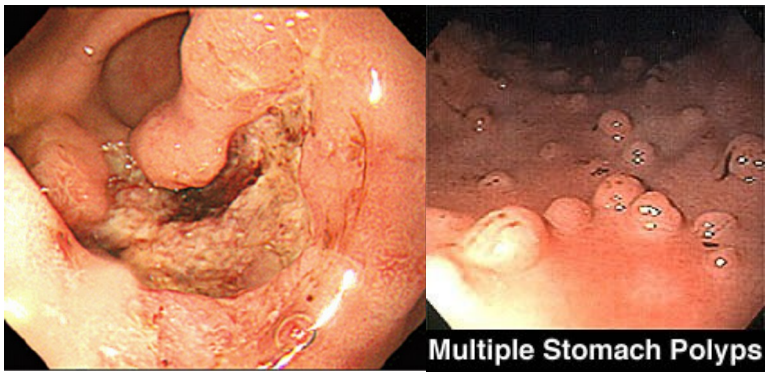

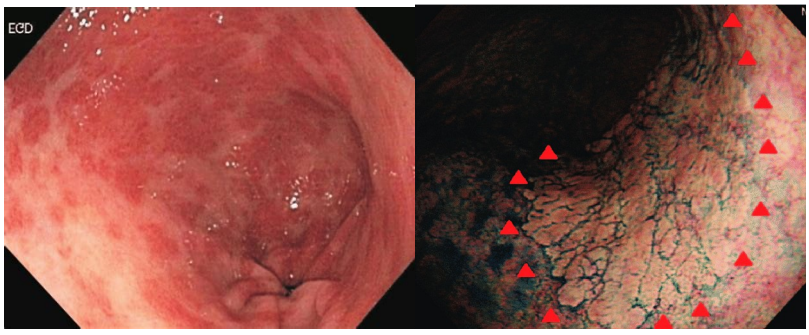

Figure 1: Different morphologies of gastric cancer

Endoscopic images taken from the upper GI tract depicting different morphologies of gastric cancer **A)** Ulcerating masses (Hyung Jun Chu) **B)** Polypoids (Medword) **C)** Linitis plastica (Vincent, Paul Co.) **D)** Superficial spread (Kyon Joo Lee).

The presence of gastric cardia is often asymptomatic until reaching advanced stages of the disease. In general, symptoms are nonspecific and the location of the tumor determines what symptoms are presented. When patients do express symptoms, they often have indigestion, nonspecific stomach pain, anorexia, weight loss, and early satiety (Tierney et al., 1999**).** These symptoms are relatively easy to relieve initially

with over the counter drugs and could potentially delay correct diagnosis of the disease. When the patient shows these symptoms, they're more likely to have advanced to an incurable state at the time of presentation. Approximately 50% of those who are diagnosed with gastric cancer have progressed beyond their initial locoregional confines. Of that 50%, only one-half of those with sustained locoregional tumor involvement can have a potentially curative surgical resection (Mansfield F., Paul, 2017).

The diagnosis of gastric cancer

When gastric cancer is suspected in a patient, a quick diagnostic evaluation should be made for prompt, appropriate action. There currently are two main diagnostic techniques in practice: endoscopy and barium studies. Endoscopy is a highly invasive and costly procedure used to investigate suspicious gastric, esophageal and duodenal lesions. It's a nonsurgical procedure where an endoscope, a flexible tube with a light and camera, is passed through the upper GI tract. Any visible suspicious lesion is biopsied and examined, and often has a 70% sensitivity for diagnosing the existing cancer. If there are six additional biopsies from the margin and base of the initial sample, sensitivity jumps to 98% (Graham, DY, 1982). This increase in sensitivity shows that it is essential to take various biopsies from surrounding benign appearing ulcers in order to increase accurate diagnosis. However, risks to this procedure include perforation, infection, internal bleeding and reaction to sedation.

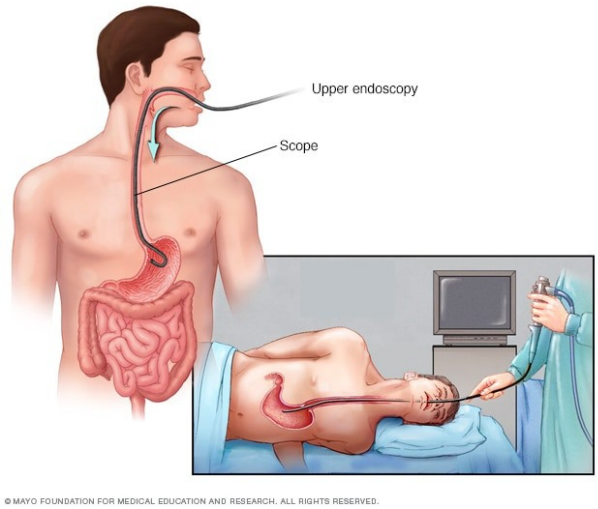

Figure 2: Endoscopy procedure

A schematic depicting an endoscopic procedure. The endoscope is inserted through the mouth and down the esophagus to view the upper GI tract and potentially biopsy suspicious lesions (MayoClinic.com).

An alternative to endoscopy is a barium upper gastrointestinal series. Barium sulfate is swallowed and tracked by a radiologist on an X-ray. Abnormalities such as esophageal narrowing, hiatal hernias, abnormally large veins, ulcers, tumors, polups, and gastroesophageal reflux disease can be detected (Thangavelu-Veluswamy, Arasi) Barium swallow tests are unreliable in detecting small lesions and in distinguishing the differences in benign and malignant ulcerations (Tierney, 1999). Additionally, this test tends to produce up to 50% false negatives in various cases (Dooley, CP, 1984).

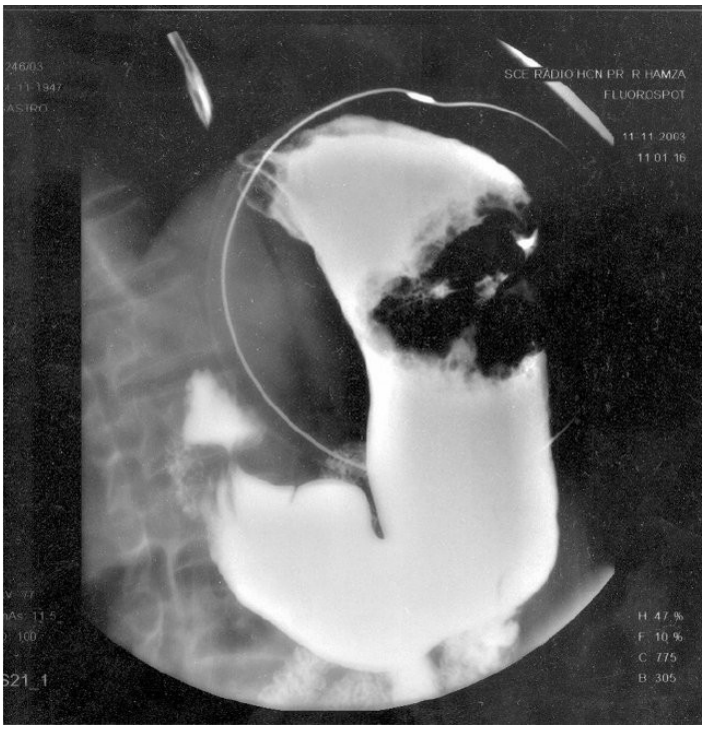

Figure 3: Barium swallow study image

An x-ray examination of a barium swallow study depicting a protruding ulcerated tumor (Issam M'Sakni, 2007).

Current methods for gastric cancer screening and diagnosis are either invasive and potentially harmful, or minimally invasive and inaccurate. This poses a problem for both high risk patients and those in the earlier stages of gastric cancer. Without a minimally invasive and accurate early screening method for gastric cardia, successful treatment and curing becomes less likely.

The cellular basis of cancer

Early tumor cells contain an aberrant and heritable change in its genes. While it is possible that epigenetic changes can alter gene expression in tumor cells, these somatic mutations are seemingly fundamental and universal in cancer. When these mutations arise, it becomes increasingly more likely that a gradual accumulation of

mutations in various genes will occur in tumor progression. This establishes different stages of the disease, depending on the number of changes in the cancer cells. For gastric cancer, these stages are based on tumor, node, and metastasis (TNM) classifications. Some changes in cell behavior that arise from carcinogenesis include an altered control of growth, sugar metabolism, and ability to withstand stress and damage to DNA (Alberts, Bruce et al. 2015). Along with internal changes, there were external cell surface changes found with the progression of carcinogenesis. In a study conducted by Mateusz Bujko et al., it was found that of 20 genes associated with cell-cell adhesion, cadherin genes CH43 and CDH1 increased in tumor tissue, along with a decrease in adherens junction genes CDH19 and PTPRF (Bujko, Mateusz et al., 2015).

Cell-Matrix adhesions

Cell-matrix junctions are a class of cell surface structures composed multiple protein complexes that provide adhesion between a cell and the extracellular matrix. They're abundant in all epithelial tissues, and are essential for providing tissue structure. These cell-matrix junctions have the ability to sense mechanical forces acting upon them (Alberts, Bruce). Cells that are attached to a tense matrix that resist the pull of cell-matrix junctions, the cell-matrix junction can sense the resulting rigidity and adjust by triggering a response to recruit integrins and other cell-surface proteins to increase the cell-junction's ability to undergo the tension (Alberts, Bruce). This overall mechanism allows a cell to adjust to attach to a variety of different matrices.

Carbon nanotubes as a cancer screening surface

With a need for a less invasive and more reliable method to screen for the presence of gastric cancers, an investigation into nanomaterials seems attractive. In general, the transformation of a normal cell into a cancerous one can be characterized as cytoskeletal changes, nuclei changes, enzymatic changes, and cell adhesion and motility changes (Adami, OA, 2002). The alterations in the cytoskeleton and in cell adhesion and motility change the internal structure and behavior of cell-cell interactions. Generally, there's reduced cell-cell and cell-extracellular matrix adhesion, promoting formation of cellular masses. As a generalization, cancer cells become more deformable than their normal counterparts. Nanomaterials have the potential to interact with cells more specifically than current diagnostic and screening methods. Additionally, if nanomaterials can effectively screen for or diagnose cancer in vitro then they are less invasive and harmful to patients. For the purposes of this investigation, carbon nanotubes (CNTs) will be the nanomaterial used for investigating cancer cell entrapment. CNTs are long tubes composed of carbon with diameters that measure in nanometers. They can be synthesized using arc discharge, laser ablation, high-pressure carbon monoxide disproportionation, and chemical vapor deposition. CNTs grown by chemical vapor deposition will be the primary nanomaterial used. The molecular structure of the CNTs allowing for a high aspect ratio and high tensile strength may prove to be useful for cancer cell screening. The tubular shape, nanometric diameter and variably long length lend to their fibrous character, mimicking protein fibers within the extracellular matrix (ECM) and potentially stimulating cellular growth (Price L., Rachel, 2003).

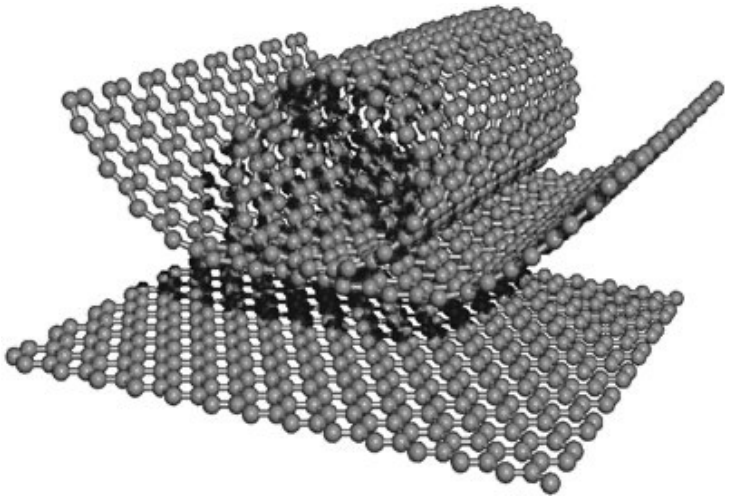

Figure 4: The basic structure of a carbon nanotube

A schematic of how a graphene sheet could be rolled up, forming a single walled carbon nanotube (Nanowerk).

In 2012 Mohammad Abdolahad et al. investigated the growth responses of two colon cancer cell lines at different metastatic grades on a multiwalled carbon nanotube surface (M. Abdolohad, 2012). The CNT-holding substrates were held at a 45^{o} angle and had cell solution flowed onto it from 2.5 cc/min to 20 cc/min. A special closed loop circulating mechanism controlled the cell solution flow on top of a shaker solution. Abdolahad found that the higher metastatic grade cell line (SW-48) became entrapped more frequently on the CNT surface compared to the other (HT-29). There was a 40% increase of entrapment, which Abdolahad credited to the increased deformability of high metastatic grade samples.

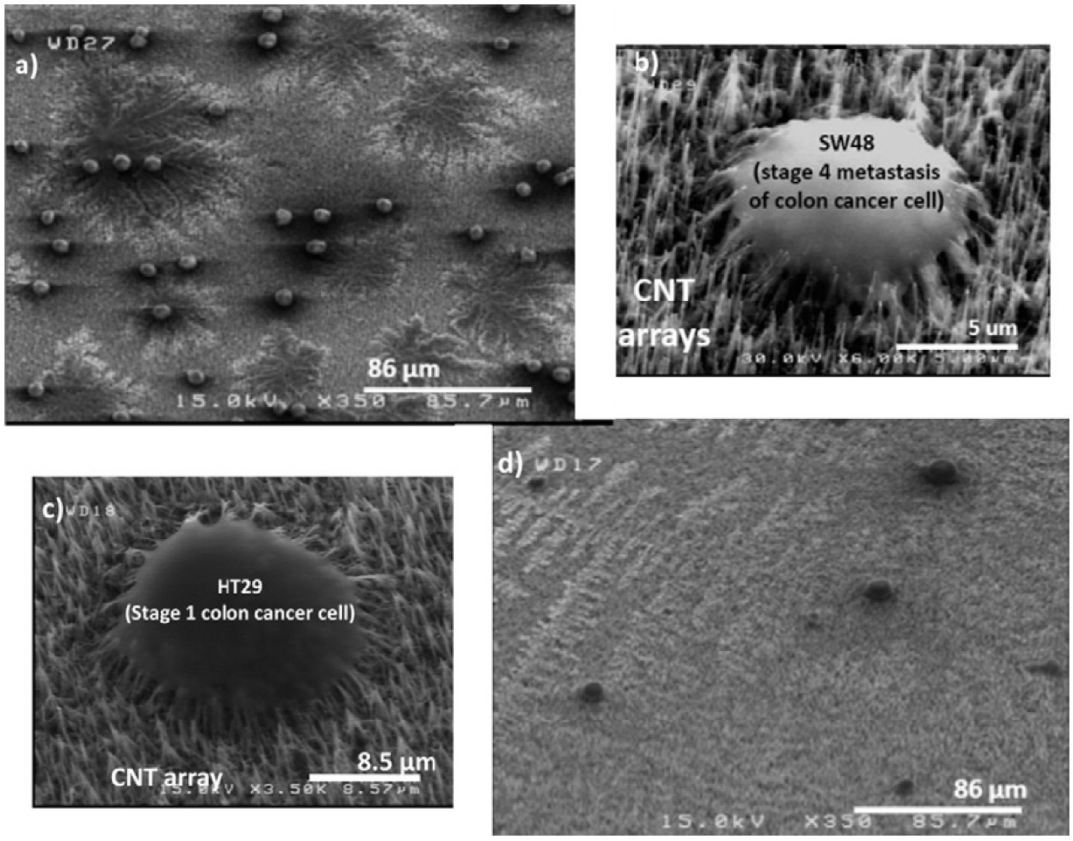

Figure 5: Cancer cell entrapment on carbon nanotubes

SEM images taken during the cellular entrapment experiment (Abdolohad) A) Trapped SW-48 cells on a CNT substrate B) Single SW-48 cell trapped on CNTs C) Single cell of HT-29 trapped on CNTs D) Trapped HT-29 cells on a CNT substrate in the same solution concentration and flow rate (2.5 cc/min) and array area (0.5 cm2) as SW-48 cells. The fraction of entrapped cells increased with higher metastatic grade.

Another study conducted by F. Fachin with MIT found that bioparticle capture in a nanostructure could be increased by incorporating a nanoporous feature onto the surface. The study in question focused on using patterned vertically aligned carbon nanotubes (VACNTs) on a silicon oxide substrate into columns spaced at 80 nm, and functionalized via wet chemistry to increase porosity. Fachin then used a pressurized introduction of *Escherichia coli* and different sized beads into the VACNT substrate. To

observe the amount of captured *E. Coli*, Fachin used fluorescent imaging. In summation, the experiment showed that cellular capture could be controlled by adjusting the functionalization of the CNT surface and by adjusting the porosity as well. They concluded that patterned CNT features could potentially be used as filters to mechanically isolate bioparticles based on their relative size to inter-CNT spacing. This method of controlling the porosity and adherence to a VACNT surface provides a potential means of controlling what sized bioparticle becomes trapped on the substrate.

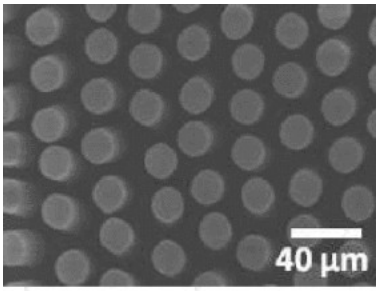

(a) SEM of an "as-grown" array of cylindrical VACNT pillar features

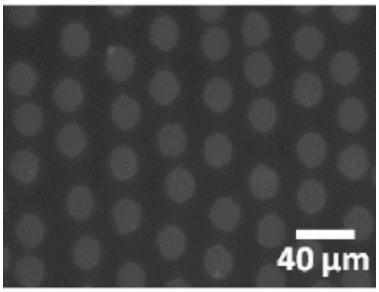

(b) 40nm virus-like beads are captured inside the VACNT pillar features.

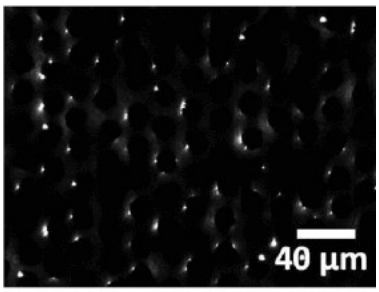

(c) 1μm bacteria-like beads accumulate on the pillar features' external surfaces.

Figure 6: Nanoporous structure capturing bioparticles

Examples of different sized bioparticle beads isolated on a CNT array using nanoporous features.

Based off of these previous studies, there appears to be great merit in using a CNT surface as a cancer screening or diagnostic method.

Methods

Patterning

The carbon nanotube surface was patterned as a >1 cm^2 checkerboard. Each square totaled to a surface area of 1 mm^2. The pattern was designed in the CAD software CleWin5, and saved as a .cif.

Photolithography

A 2 inch-diameter silicon oxide wafer was prepared for photolithography by first sonicating it in acetone for 10 minutes and rinsing with isopropyl alcohol. The wafer was heated at 400C for 15 minutes and then exposed to hexamethyldisilazane for 20 minutes to promote photoresist adhesion. The surface of the wafer was evenly coated in AZ1512 positive tone photoresist by spin-coating at 3000rpm for 30s. The photoresist was soft-baked for 2.5min at 105C. The sample was exposed using a 405nm laser in a Suss MicroTech Direct Write Laser Lithography System. After writing the pattern, the wafer was placed on a hot plate for 1 minute at 105C and then developed in AZ 300 MIF developer for 1 minute. The wafer was then hard-baked for 2 minutes at 105C and then stored in a nitrogen environment for later use.

CNT growth

For CNT growth, a seed layer of 3nm of Al and 6nm of Fe was deposited on the surface of the wafer using thermal evaporation. Lift off of the photoresist was performed in acetone. The wafer was scribed into approximately 1 cm^2 chips using a

diamond scribe. The resulting wafers were cleaned in acetone for 10 minutes and rinsed with IPA to clean off any residual debris. The chips were placed into a chemical vapor deposition furnace and CNTs were grown at 650ºC in the presence of Argon, Hydrogen, and Ethylene gas.

Cells and Reagents

Adherent gastric adenocarcinoma cells (AGS: ATCC CRL-1739) were cultured in F-12K medium supplemented 10% fetal bovine serum (FBS). Cells were subcultured by removing and discarding spent media, washing with PBS, followed by a 5-10 minute incubation in 0.05% trypsin-EDTA to further dislodge cells from the flask. F-12K was added to a T-75 flask with a million of cells was added. The cells were incubated at 37C in 5% CO_2.

Semi-adherent gastric carcinoma cells (KATO III: ATCC HTB-103) were maintained in Iscove's Modified Dulbecco's medium (IMDM) supplemented with 20% FBS. Cells were subcultured by first collecting the spent media containing the suspended cells into a 15 mL conical tube. Cells were washed with PBS, and 2 mL of Trypsin-EDTA was added for 5-10 minutes to further dislodge cells from the flask. 4 mL of growth media was added and aspirated. To remove the growth media and Trypsin-EDTA serum from the solution, the cell suspension was added to the centrifuge tube and centrifuged for 10 minutes at 125 x g. Then the supernatant was discarded and cells resuspended in fresh growth medium. Appropriate aliquot of cells was added to a T-75 flask. Cells were incubated at 37C in 5% CO_2.

Seeding on the Carbon Nanotube Forest

KATO III cells were collected from a T-75 flask which was washed with 1 mL 1X PBS. The collected KATO III cells were centrifuged at 125 x g for 10 min. 1 mL of 0.05% Trypsin was added to the T-75 to enzymatically dissociate the cells. The flask was incubated at 37C for 5 minutes, then the cells were resuspended with 4 mL of F-12K media. A 10 µL sample of cells was taken to be counted on a hemocytometer. Based on the calculated concentration of cells in the flask, the resulting cell suspension is added to the appropriate amount of medium to create a concentration of 250 thousand cells. The sample would be serially diluted to concentrations 125 thousand, 62 thousand, 31 thousand cells in their respective chamber slides in triplicate. Cells were allowed to grow for 24 hours.

Confluent AGS cells were aspirated in a T-75 flask and washed with 1 mL 1X PBS. 1 mL of 0.05% Trypsin was added to the T-75 to enzymatically detach cells from their adhesion to the flask and to themselves. The flask was then incubated at 37C for 5 minutes. The cells were then resuspended with 4 mL of F-12K media to make a 5 mL cell suspension. A sample of cells was extracted to be counted on the hemocytometer. Based on the calculated concentration of cells in the flask, the resulting cell suspension would be added to the appropriate amount of medium to create a concentration of 250 thousand. The sample would be serially diluted to concentrations 125 thousand, 62 thousand, 31 thousand cells in their respective chamber slides. Cells were allowed to grow for 24 hours.

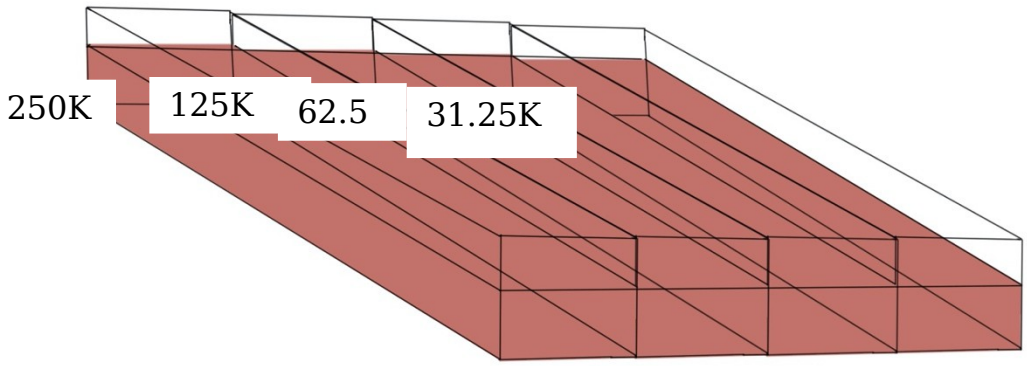

Figure 7: Cell culture set up

Cells and media were grown in Falcon 4-chamber culture slides at concentrations 250 thousand, 125 thousand, 62 thousand, and 31 thousand.

Immunofluorescence Staining

After 24 hours of growth, the media was aspirated from each well and the cells were washed with PBS. The cells were fixed with 4% PFA in PBS for 10 min at room temperature. The PFA was removed and each sample was washed with PBS 3 times for two minutes each. Samples were then washed with a PBS/DAPI mix, followed by an additional PBS wash. After the washes, all of the replicates were taped onto a glass slide and labeled appropriately (i.e.: AGS 250K). N-propyl gallate was then pipetted on top of the chips and covered with a cover slip. The edges were sealed by inserting nail polish underneath the coverslips and left to dry. To further adhere the coverslips, the edges were taped down.

Imaging the Cells

Cells were imaged using NIS Elements program. At 10X magnification 200 ms exposure and 9.3x gain, the chips were centered on the target material. A picture was taken after bringing the photo into focus. 3 different photos were captured of both materials on different areas of the chip.

Counting the Cells

Images were analyzed in FIJI images were un-stacked to only feature the DAPI channel. Each photo was cropped to only feature the material being examined. If edges were difficult to detect, the image was viewed in NIS Elements Viewer and contrast adjusted. After cropping the image, it was turned into a binary image and watersheded and saved as a TIFF image. Cells were then auto counted by defining circularity as 600-50000 pixels. Leftover uncounted cells or incorrectly counted cells were then manually counted and added to the overall value. This value was saved as a .nd2 file.

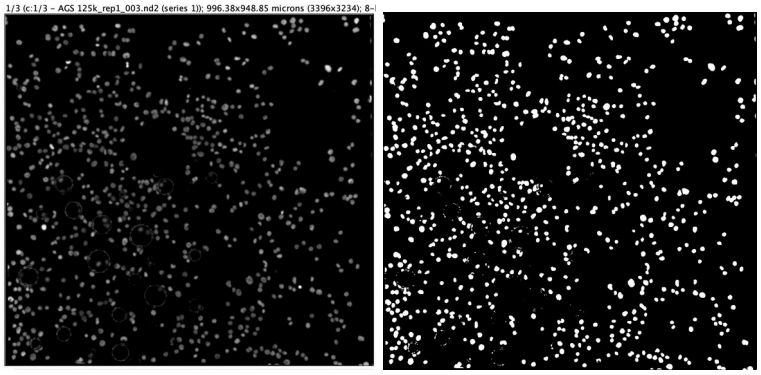

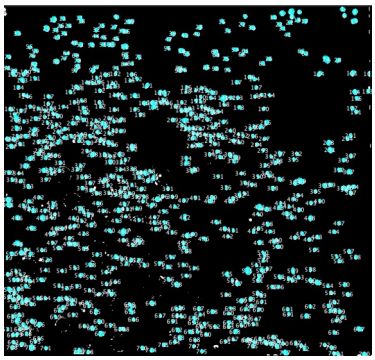

Figure 8: FIJI image analysis of an example photo

Schematic of FIJI image analysis. A) The raw .nd2 file cropped to fit the material's surface area B) The .nd2 image turned into a binary image C) The autocounted cells according to the defined pixel range (600-5000), and overlayed with counting masks. Cells that were visibly not counted or areas that were not stained nuclei were manually input into a separate cell counter and added to the overall total.

Statistical analysis

Total cell count values for each cell type and concentration were analyzed by a student's t-test run in GraphPad Prism software. Significance was determined by the P-value by the following scale: *=$p<0.05$, **= $p<0.005$.

Results

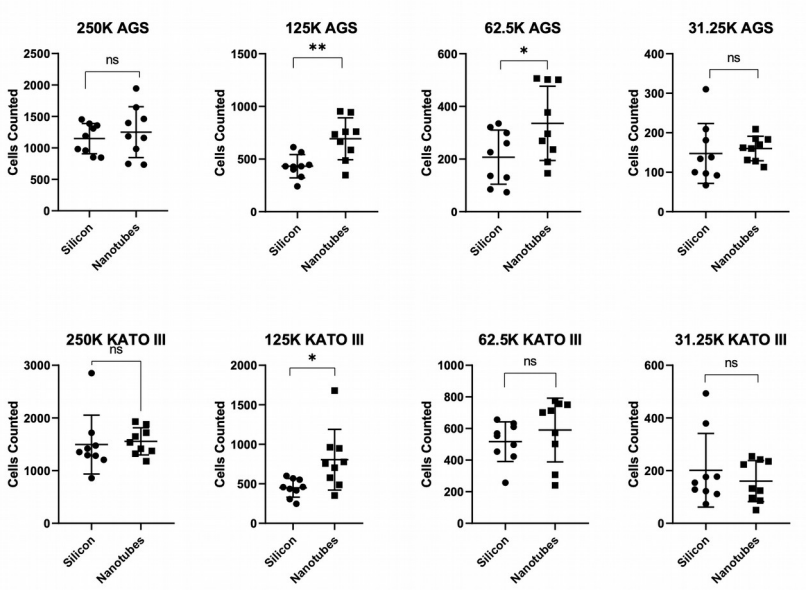

Figure 9: Results of cell counts at each concentration

Individual cell counts displayed in a box and whisker plot, comparing cell entrapment differences between the silicon oxide and CNT substrates. P-value tests ran for each cell line and density are as follows: AGS 250 thousand (p-value=0.522); AGS 125 thousand (p-value=0.003); AGS 62 thousand (p-value=0.042); AGS 31 thousand (p-value=0.652); KATO III 250 thousand (p-value=0.724); KATO III 125 thousand (p-value=0.017); KATO III 62 thousand (p-value=0.365); KATO III 31 thousand (p-value=0.451).

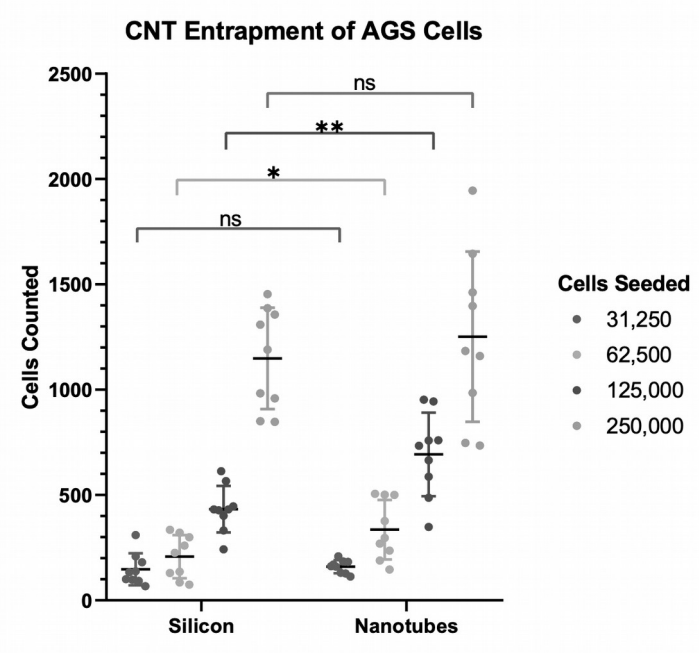

Figure 10: AGS cell counts

All AGS cell counts displayed in a box and whisker plot on the same y-axis scale.

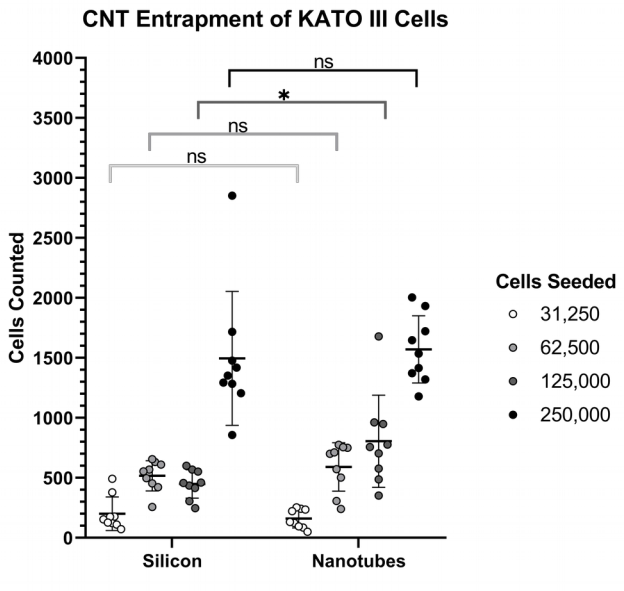

Figure 11: KATO III cell counts

All KATO III cell counts displayed in a box and whisker plot on the same y-axis.

We found no significance in cell entrapment between the silicon oxide and CNT substrate for AGS in the seeding densities 250 thousand and 31 thousand cells. There was also no significance in KATO III capture rate between the silicon oxide and CNT for seeding densities 250 thousand, 62 thousand, and 31 thousand cells. There was significance in cell capture rate for AGS densities 125 thousand (p value=0.003359) and 62 thousand (p value=.042211). There was significance in cell capture rate for KATO III density 125 thousand (p value=0.017). Overall, there was more significance in cell entrapment for the AGS cell line.

Discussion

Results discussion

With a majority of the KATO III concentrations showing no significant cell entrapment difference and with a p-value= 0.017 for the 125 thousand concentration, there appears to be no preferential affinity. This could potentially be attributed to its partial suspension and partial adherent nature. According to ATCC.org, the cell line was derived from a metastatic site at a pleural effusion from the lungs, the supraclavicular and axillary lymph nodes, and the Douglas cul-de-sac (ATCC, 2020). It may have been an inappropriate cell line to use for the scope of this research. The aim of this experiment was to test if there was a difference in entrapment for gastric cancer cells. Because this cell line isn't fully adherent, it didn't fully provide insight into the entrapment of those cells on a CNT vs. silicon oxide substrate. It would have been more worthwhile to compare a different cell line that was at a different fully adherent metastatic grade than the AGS cell line. The AGS cell line appears to express an affinity for a CNT substrate over a silicon oxide substrate in the 62.5 thousand-125 thousand concentration range. This range shows there may be a dynamic interplay between the CNTs and the cell surface. The exact phenomenon of what is occurring at the cell surface is not known, but it would be worthwhile to repeat this experiment and attempt to replicate the results.

Next steps

Another feature that would be valuable in investigating would be the overall spatial distribution of the adherent gastric cancer cells over a selected line spanning across a silicon oxide and CNT surface. A spatial profile of cells occupying both materials in a clearly defined rectangular area would be analyzed in FIJI. A plot featuring the number of cells over distance would be made by taking a binary image with both materials and analyzing the gray value over distance in pixels. By analyzing both materials in this manner, it would provide greater insight into how the adherent cells are spatially distributed.

Additional repetitions of this experiment should also be done to test if the results can be replicated. KATO III's would not be used as a cell line for experiment repetition, as it has been demonstrated to be an inappropriate line to use for the scope of this study. The next immediate step for this research would be to repeat the experiment with AGS cells and NCI-N87 (ATCC CRL-5822), another adherent gastric cancer. Each replication would be done with a different batch of cells passed at different times. The procedure would otherwise remain the same. The focus would be with the same concentrations and repeated twice over to ensure repeatability. If there were a consistent entrapment difference at this concentrate range, then it would indicate that the CNTs are capturing the gastric cancer cells at a higher rate than silicon oxide. If this were to be shown, it would be worthwhile to closely observe changes in the cell membrane. Examining the potential expression changes in cell junction markers could lend insight into structural changes of cancer cells when interacting with a CNT structure.

Conclusion

In summary, this study helps provide an insight into how a CNT structure preferentially entraps adherent gastric cancer cells within a specific concentration range. This proof of concept research raised more questions on why a certain concentration range would capture a significantly larger number of cells on a CNT surface as compared to a silicon oxide structure. If there were more time to explore this subject, it would be useful to also examine other adherent gastric cancer cell lines. It would also be interesting to further explore this dynamic interplay between adherent gastric cells and a CNT surface by observing cell surface changes. Regardless, this study provides more insight into the field of using nanomaterials as a means for cell capture.

Glossary

Carbon Nanotubes: A common form of nanotube, having graphene sheets folded into perfect cylinders.

Biopsy: The removal and examination of a sample of tissue to be examined for diagnostics purposes.

Endoscopy: The internal inspection of a cavity or canal of the body by means of an endoscope.

Extracellular matrix: All of the fibrous proteins and connective tissues associated with the cell, but not a part of the cell.

Metastatic cancer: Cancer that has progressed beyond the locoregional area of the initial tumor.

Bibliography

Abdolahad, M., et al. “Vertically Aligned Multiwall-Carbon Nanotubes to Preferentially Entrap Highly Metastatic Cancerous Cells.” *Carbon*, Pergamon, 9 Jan. 2012, www.sciencedirect.com/science/article/pii/S0008622312000267.

Adami, Hans-Olov, et al. *Textbook of Cancer Epidemiology*. Oxford University Press, 2018.

Alberts, Bruce, et al. *Molecular Biology of the Cell*. Garland Science, 2015.

Bujko, Mateusz, et al. “Expression Changes of Cell-Cell Adhesion-Related Genes in Colorectal Tumors.” *Oncology Letters*, D.A. Spandidos, June 2015, www.ncbi.nlm.nih.gov/pmc/articles/PMC4473523/.

“Cancer Today.” *Global Cancer Observatory*, gco.iarc.fr/today/online-analysis-pie?v=2018&mode=cancer&mode_population=continents&population=900&populations=900&key=total&sex=0&cancer=39&type=0&statistic=5&prevalence=0&population_group=0&ages_group[]=17&nb_items=7&group_cancer=1&include_nmsc=1&include_nmsc_other=1&half_pie=0&donut=0&population_group_globocan_id=.

Chu, Hyung Jun. “Research Gate.” *Research Gate*.

Dooley, C P, et al. “Double-Contrast Barium Meal and Upper Gastrointestinal Endoscopy. A Comparative Study.” *Annals of Internal Medicine*, U.S. National Library of Medicine, Oct. 1984, www.ncbi.nlm.nih.gov/pubmed/6383166.

“Mayo Clinic.” *Mayo Clinic*.

Fachin, F, et al. “Integration of Vertically-Aligned Carbon Nanotube Forests in Microfluidic Devices for Multiscale Isolation of Bioparticles - IEEE Conference Publication.” *IEE Explore*, ieeexplore.ieee.org/abstract/document/5690852.

Graham, D Y, et al. “Prospective Evaluation of Biopsy Number in the Diagnosis of Esophageal and Gastric Carcinoma.” *Gastroenterology*, U.S. National Library of Medicine, Feb. 1982, www.ncbi.nlm.nih.gov/pubmed/7054024.

Helicobacter and Cancer Collaborative Group. “Gastric Cancer and Helicobacter Pylori: a Combined Analysis of 12 Case Control Studies Nested within Prospective Cohorts.” Gut, U.S. National Library of Medicine, Sept. 2001, www.ncbi.nlm.nih.gov/pubmed/11511555.

"KATO III (ATCC® HTB-103™)." KATO III ATCC ® HTB-103™ Homo Sapiens Stomach; Derived From, www.atcc.org/products/all/HTB-103.aspx.

Lee, Kyoon Joo. "Research Gate." Research Gate.

M'sakni, Issam. "Research Gate." Research Gate.

"Medword." Medword.

"A Schematic Depicting How a Graphene Sheet Could Be Rolled up to Form a Carbon Nanotube." Nanowerk.

Papaxoinis, George, et al. "Primary Gastrointestinal Non-Hodgkin's Lymphoma: a Clinicopathologic Study of 128 Cases in Greece. A Hellenic Cooperative Oncology Group Study (HeCOG)." *Leukemia & Lymphoma*, U.S. National Library of Medicine, Oct. 2006, www.ncbi.nlm.nih.gov/pubmed/17071488.

Price, Rachel L, et al. "Selective Bone Cell Adhesion on Formulations Containing Carbon Nanofibers." *Biomaterials*, U.S. National Library of Medicine, May 2003, www.ncbi.nlm.nih.gov/pubmed/12615478.

"Stomach Cancer Statistics: Gastric Cancer Statistics." *American Cancer Society*, www.cancer.org/cancer/stomach-cancer/about/key-statistics.html.

"Stomach Cancer Statistics: Gastric Cancer Statistics." *American Cancer Society*, www.cancer.org/cancer/stomach-cancer/about/key-statistics.html.

Thangavelu-Veluswamy, Arasi. "What Is a Barium Swallow Test? Procedure, Side Effects, Prep." *EMedicineHealth*, EMedicineHealth, 4 Oct. 2019, www.emedicinehealth.com/barium_swallow/article_em.htm.

Tierney, Lawrence M., et al. *A Lange Medical Book Current Medical Diagnosis & Treatment 1999*. Appleton & Lange, 1999.

Vincent, Paul Co. "Research Gate." *Research Gate*.

Wardle, et al. "Integration of Vertically-Aligned Carbon Nanotube Forests in Microfluidic Devices for Multiscale Isolation of Bioparticles." *Integration of Vertically-Aligned Carbon Nanotube Forests in Microfluidic Devices for Multiscale Isolation of Bioparticles*, Institute of Electrical and Electronics Engineers, 1 Nov. 2010, dspace.mit.edu/handle/1721.1/65845.

Zali, Hakimeh, et al. "Gastric Cancer: Prevention, Risk Factors and Treatment." *Gastroenterology and Hepatology from Bed to Bench*, Research Institute for Gastroenterology and Liver Diseases, 2011, www.ncbi.nlm.nih.gov/pmc/articles/PMC4017429/.

Zali, Hakimeh, et al. “Gastric Cancer: Prevention, Risk Factors and Treatment.” *Gastroenterology and Hepatology from Bed to Bench*, Research Institute for Gastroenterology and Liver Diseases, 2011, www.ncbi.nlm.nih.gov/pmc/articles/PMC4017429/#CIT0013.